Microbial sulfur cycling across a 13,500-year-old lake sediment record

Jasmine S. Berg[1*], Paula C. Rodriguez[2], Cara Magnabosco[2], Longhui Deng[3a], Stefano M. Bernasconi[2], Hendrik Vogel[4], Marina Morlock[4b], Mark A. Lever[3c]

[1]Institute of Earth Surface Dynamics, Department of Geosciences and Environment, University of Lausanne, 1015 Lausanne, Switzerland

[2]Department of Earth and Planetary Sciences, ETH-Zurich, 8049 Zurich, Switzerland

[3]Institute of Biogeochemistry and Pollutant Dynamics, Department of Environmental Systems Science, ETH-Zurich, 8049 Zurich, Switzerland

[4]Institute of Geological Sciences & Oeschger Centre for Climate Change Research, University of Bern, 3012 Bern, Switzerland

*corresponding author: jasmine.berg@unil.ch

[a] Present address: School of Oceanography, Shanghai Jiao Tong University, Shanghai 200240, China

[b] Present address: Department of Ecology and Environmental Sciences, Umeå Universitet, 901 87 Umeå, Sweden

[c] Present address: Marine Science Institute, University of Texas at Austin, Port Aransas, TX 78373, USA

keywords: *sulfur cycling, sulfur isotopes, organic sulfur, early diagenesis, lake sediment, meromictic, Holocene, euxinic*

ABSTRACT

The sulfur cycle is very important in lake sediments, despite the much lower sulfate concentrations in freshwater than seawater. To date, little is known about the formation and preservation of organic and inorganic sulfur compounds in such sediments, especially in the sulfate-depleted subsurface. Here we investigated the fate of buried S-compounds down to 10-m sediment depth, which represents the entire ~13.5 kya sedimentary history, of the sulfate-rich alpine Lake Cadagno. Chemical profiles of sulfate and reduced sulfur reveal that sulfate from lake water is depleted at the sediment surface with the concomitant formation of iron sulfide minerals. An underlying aquifer provides a second source of sulfate and other oxidants to the deepest and oldest sediment layers generating an inverse redox gradient with ongoing sulfate consumption. The isotopic offsets between pools of humic acid-sulfur, acid-volatile sulfur (AVS) and chromium-reducible sulfur (CRS) in both surface and deep sediments suggest differential timing of formation, with sulfide oxidation to sulfur/polysulfides playing an integral role in organic matter sulfurization. Although sulfate is depleted in the central part of the sediment column, *dsrB* gene libraries reveal a potential for microbial sulfur reduction throughout the sediment column, with sequences in sulfate-depleted layers being dominated by Chloroflexota. Collectively, our data indicate an active sulfur cycle that is driven by uncultivated microorganisms in deep sulfate-depleted sediments of Lake Cadagno.

1. INTRODUCTION

The biological sulfur cycle exerts an important control on organic matter burial and thus plays a major role in the global cycling of carbon, oxygen, nitrogen and iron. In anoxic marine sediments, microbial reduction of sulfate (SO_4^{2-}) to hydrogen sulfide (ΣH_2S) is quantitatively the most important respiration reaction, remineralizing upwards of 30% of the total organic carbon flux to the seafloor (Jørgensen, 1982; Bowles et al., 2014; Baloza et al., 2022). Even in freshwater systems, where sulfate concentrations are typically 100-1,000 times lower than in seawater, high rates of microbial sulfate reduction can be sustained by rapid reoxidation of ΣH_2S by Fe^{III}, Mn^{IV}, and possibly by redox-active organic substances, e.g. certain humic acids (Pester et al., 2012; Hansel et al., 2015).

Sulfur isotopic fractionation provides important insights into microbial sulfur cycling in the past and present by recording signatures of these processes within different sulfur pools, including sulfide minerals. The preferential reduction of ^{32}S- over ^{34}S-sulfate generates isotopic fractionations of 3 to 75 ‰ between sulfate and hydrogen sulfide in microbial cultures (e.g. (Kaplan and Rittenberg, 1964; Habicht and Canfield, 1997; Detmers et al., 2001; Rudnicki et al., 2001; Wortmann et al., 2001; Brunner and Bernasconi, 2005; Sim et al., 2011; Bradley et al., 2016)). Nonetheless, the dynamics and controls on the magnitude of sulfur isotope fractionation by sulfate reducing microorganisms have proven to be complex to understand in the environment. While pyrite $\delta^{34}S$ values supposedly record the S isotopic composition of sulfide in porewater fluids, major isotopic differences (between 10 and 40‰) have been observed between coexisting sedimentary pyrite and dissolved H_2S (Chanton et al., 1987; Canfield et al., 1992; Brüchert and Pratt, 1996; Raven et al., 2016; Lin et al., 2016). These discrepancies have been explained by processes such as sediment remobilization, bioturbation, or post-depositional sediment-fluid interactions (Jørgensen et al., 2004; Fike et al., 2015). While

the $\delta^{34}S$-composition of pyrite has been widely used to interpret global changes in the Earth's sulfur cycle or microbial metabolic pathways, an earlier body of work (e.g., Schwarcz and Burnie, 1973; Goldhaber and Kaplan, 1975, 1980; Maynard, 1980) showed that $\delta^{34}S$-isotopic variations in marine sediments are largely controlled by local physical factors, such as sedimentation rate, along with the supply of Fe and OM. In open systems, the sulfate pool is constantly replenished with light ^{32}S-sulfate, whereas under conditions of rapid sedimentation, sulfate in sediment pore spaces is sealed off from overlying waters and the sulfate pool undergoes Rayleigh distillation (Hartmann and Nielsen, 2012). Closed versus open system sulfate reduction can thus explain the large variability in observed fractionations between sulfide and sulfate, which is recorded in sediments by authigenic pyrite (e.g., (Och and Shields-Zhou, 2012; Bryant et al., 2023)).

While pyrite is the dominant S pool in most marine sediments, the biggest S pool in many freshwater sediments is organic S (Mitchell et al., 1981; Nriagu and Soon, 1985; Losher, 1989; Urban et al., 1999). This organic S originates from both the settling of seston material and the microbial reduction of water column-derived sulfate to hydrogen sulfide, which then reacts with sedimentary organic matter (David and Mitchell, 1985; Rudd et al., 1986; Losher, 1989; Putschew et al., 1996; Damste et al., 1998). The sulfurization of organic matter tends to promote organic matter resistance to microbial degradation and is thus believed to contribute substantially to long-term preservation of organic carbon in sediments (Damsté and De Leeuw, 1990; Hebting et al., 2006), and to petroleum formation (Orr and Damsté, 1990). Though it is likely that some microorganisms are capable of degrading fractions of this organic S pool, their activity and identity is unknown.

Recently, the metabolic capacity for sulfur cycling has been expanded to new phylogenetic groups based on the detection of specific marker genes for sulfur cycling within these taxa (e.g., Anantharaman et al., 2018). Although the presence of such genes must be

interpreted with caution, their distribution across environments can help illuminate the distributions of putative sulfur reducing and sulfur oxidizing microbial communities. Thiosulfohydrolase of the sulfur oxidation (Sox) enzyme system (*sox*B) is one such marker gene and has been widely employed to characterize the diversity of sulfur-oxidizing bacteria (SOB) (Meyer et al., 2007). Another example is dissimilatory sulfite reductase (*dsr*AB), an enzyme that catalyzes the reduction of sulfite to sulfide and is used by all known sulfate reducers (Klein et al., 2001).

Because low rates of microbial sulfur cycling continue in sulfate-depleted marine sediments (Holmkvist et al., 2011; Treude et al., 2014; Brunner et al., 2016; Pellerin et al., 2018a), such processes may likewise occur in sulfate-depleted sediments of lakes and leave a lasting imprint on the lake sulfur geochemical record. Here we investigate the potential for microbial sulfur cycling in Lake Cadagno, which is an intermediate system between freshwater and seawater, due to its elevated sulfate concentrations (1-2 mM). We combine chemical and isotopic analyses of major S and C phases with quantification and sequencing of S-cycling genes (*dsr*B, *sox*B) to investigate S cycling across the complete ~13.5 kya sedimentary history of Lake Cadagno.

METHODS

2.1 Geological setting and sampling

The meromictic Lake Cadagno, located in the Swiss Alps, contains 1-2 mM dissolved sulfate, which originates from the dissolution of sulfate-bearing dolomite bedrock via subaquatic springs. Since its formation ~13.5 kya, Lake Cadagno has undergone a complex redox history, transitioning from seasonal stratification around 12.5 kya to complete euxinia about 10.9 kya (Wirth et al., 2013; Berg et al., 2022). Preliminary analyses of sulfur phases in surface and deep sediments (Berg et al., 2022) reveal two sulfate depletion zones (SDZ). For

high-resolution analyses, short cores were retrieved from the deepest part of the lake (46.55060 N and 8.71201 E) using a UWITEC gravity corer fitted with plastic liners with 1 m length and 9 cm inner diameter. Deep cores of 3-m long and 6-cm diameter core sections were recovered using a percussion piston-coring system (Uwitec, AT). More details are provided in (Berg et al., 2022). Cores from three parallel boreholes were reserved for non-destructive imaging, porewater extraction, and solid-phase analyses, respectively.

In brief, porewater was extracted using syringes connected to Rhizons (0.2 μm pore size, Rhizosphere) pre-flushed with 2–3 ml of pore water to remove contaminant air. Porewater was then distributed into separate vials with appropriate fixatives for downstream analyses described below. For solid-phase samples, windows were cut into the core liners using a hand-held vibrating saw and potentially contaminated sediment in contact with the liner was scraped away. Samples were then taken using sterile, cut-off syringes and frozen (-20°C) in separate aliquots for DNA and solid-phase extractions.

Additional samples for sulfate isotope analyses were obtained in June 2020 from one surface spring (at SwissGrid coordinates 2'697'763, 1'155'959) and one subaquatic spring at approximately 5 m depth (2'697'521, 1'156'044) located on the south side of the lake.

Porewater samples in 1991 were also collected from a gravity core from the deepest point in the lake. Porewater was extracted using a dialysis porewater sampler (Brandl and Hanselmann, 1991) consisting of 80 x 20 x 1.5 cm Plexiglas sheets containing 41 rows of cylindrical dialysis chambers, each 1.5 cm in diameter and 1.5 cm deep. The chambers were covered on both sides with membranes held in place by 3 mm thick Plexiglas overlays. The membranes sealed the single chambers and prevented exchanges between them. Up to five individual samples of 2.6 mL can be collected from each row. Divers positioned the sampler in the sediment, leaving 10 cm extending above the sediment-water interface to collect bottom

water samples, and it was allowed to incubate for two weeks. After recovery, the water of the individual chambers was immediately extracted from the chambers with a syringe and injected in a vial containing a silver nitrate solution to precipitate silver sulfide.

2.2 Porewater and solid-phase analyses

Samples for analysis of dissolved metals (Fe, Mn) were acidified with 5 µL of 30% HCl per 2 ml to prevent precipitation and measured by inductively coupled plasma optical emission spectroscopy (ICP-OES, Agilent Technologies 5100). Samples for dissolved sulfate were immediately frozen at −20°C until analysis by ion chromatography (DX-ICS-1000, DIONEX). A part of this sample was reserved for precipitation as $BaSO_4^{2-}$ and S-isotopic analysis as described below.

The silver sulfide precipitate from 1991 porewater samples was recovered by centrifugation, dried and preserved for later sulfur isotope analysis. The remaining solution was acidified to pH<2 and sulfate was precipitated with $BaCl_2$, recovered by filtration and dried for analysis.

Total carbon (TC) and total sulfur (TS) were determined from oven-dried sediment (70°C) by EA-IRMS as described below. Total organic carbon (TOC) was determined after acid-extraction of inorganic carbon with concentrated 6 N HCl. Total inorganic carbon (TIC) was calculated as the difference between TC and TOC. Solid, reactive iron was determined on anoxically treated, freeze-dried samples by extraction with 0.25 mM HCl and subsequent photometric determination of Fe(II)/Fe(III) in the supernatant (Stookey, 1970).

2.3 Solid-phase sulfur extractions

Sequential sulfur extractions were performed on freeze-dried samples based on the protocol of Ferdelman et al. (1991). First, elemental sulfur was extracted under N_2 atmosphere three times

with degassed 100% methanol. During each step the methanol-sample mixture was sonicated for 10 min in an ice bath, centrifuged, and then the methanol was pipetted into a clean vial. Methanol extracts were analyzed by ultrahigh pressure liquid chromatography (UPLC) using a Waters Acquity H-class instrument with an Aquity UPLC BEH C18, 1.7 μm, 2.1 × 50 mm column (Waters, Japan) and a PDA detector (absorbance wavelength set to 265 nm). The injection volume was 10 μl with methanol as eluent flowing at 0.2 ml min^{-1}. Elemental sulfur eluted at 4.14 min.

Next, humic acids were extracted 3 times, or until the supernatant was clear, with degassed 0.1 M NaOH and collected in 50 ml Falcon tubes. Silicates were precipitated from the base extracts by addition of saturated NaCl solution (5 mL per 45 mL extract) and removed by centrifugation and decanting. The basic extract was acidified to pH 1.5 with concentrated HCl, allowed to stand at 4°C overnight, and centrifuged to precipitate humic acids. These were washed three times with distilled water to remove salts prior to drying and C, N, and S analysis.

Finally, acid-volatile sulfur (AVS) and chromium-reducible sulfur (CRS) were extracted from the remaining sediment using the two-step acid Cr-II method (Fossing and Jørgensen, 1989; Kallmeyer et al., 2004). For the AVS fraction, 6 N HCl was added to sediment in a reaction flask under an N_2 atmosphere and H_2S was trapped by bubbling through a 5% Zn-acetate solution for 2 h. The CRS fraction was subsequently obtained by adding 20 ml of the organic solvent dimethyl sulfoxide and 16 ml of $CrCl_2$ solution and reacting again for 2 h. AVS and CRS fractions, collected as ZnS, were quantified photometrically as above, pelleted by centrifugation, rinsed with MilliQ, and dried at 50°C prior to $\delta^{34}S$ analyses as described below.

2.4 Isotopic analyses

Isotopic compositions of sulfur in the sedimentary AVS, CRS and humic acid sulfur (HAS) fractions, and of dissolved sulfate from sediment porewater, a subaquatic spring, and

two surface springs, were determined using a Flash-EA 1112 (ThermoFisher) coupled to an isotope ratio mass spectrometer (IRMS, Delta V, ThermoFisher) by addition of vanadium pentoxide as a catalyst. Isotope ratios are reported in the conventional δ-notation with respect to the Vienna-Cañon Diabolo Troilite (VCDT) standard for sulfur. The system was calibrated for sulfur using the international standards for sulfide and sulfate: IAEA-S1 ($\delta^{34}S$ = -0.3‰), IAEA-S2 ($\delta^{34}S$ = +22.67‰), IAEA-S3 ($\delta^{34}S$ = -32.55‰) and IAEA-SO5 ($\delta^{34}S$ = +0.49‰), IAEA-SO6 ($\delta^{34}S$ = -34.05‰), NBS-127 ($\delta^{34}S$ = +21.1‰), respectively. Reproducibility of the measurements was better than 0.2‰. This method also produced the weight % sulfur in the humic acid extracts.

The 1991 samples were measured at ETH Zürich by combusting 1-2 mg of silver sulfide sealed in Quartz glass tubes with copper oxide turnings at 950 °C. The SO_2 was separated from other combustion products using a pentane-liquid nitrogen slush and was measured on a VG 903 mass spectrometer. The system was calibrated with IAEA-S1 and IAEA-S3 and NBS 28. Reproducibility of the standards $\delta^{34}S$ value was better than ± 0.3 ‰.

2.5 DNA extraction and sulfur-cycling gene analyses

DNA was extracted from frozen sediment according to the lysis protocol II of (Lever et al., 2015) as outlined in (Berg et al., 2022). The *dsr*B gene was PCR-amplified using the *dsr*B F1a-h / 4RSI1a-f primer mixtures from (Lever et al., 2013). *sox*B genes were amplified using the recently designed *sox*B-837F1a-l / *sox*B_1170R1a-g primer mixtures (Deng et al., 2022). Quantitative PCRs (qPCR) were performed on a LightCycler 480 II system using the reagent mixtures outlined in (Jochum et al., 2017). The thermal cycler settings were (1) enzyme activation and initial denaturation at 95°C for 5 min; (2) 60 cycles of (a) denaturation at 95°C for 30 s, (b) annealing at 56°C (*dsr*B) or 60°C (*sox*B) for 30 s, (c) elongation at 72°C for 25 s, and (d) fluorescence acquisition at 82°C (*dsr*B) or 86°C (*sox*B) for 5 s; and (3) a stepwise

melting curve from 60 to 95°C to check for primer specificity. Plasmids containing full-length *dsrA*B and *sox*B genes of *Desulfotomaculum carboxydivorans* and *Thiobacillus denitrificans*, respectively, were applied as qPCR standards.

*dsr*B gene sequences were phylogenetically annotated using the ARB software (www.arb-home.net) based on an updated version of the *dsr*AB database published in (Müller et al., 2015). This database was expanded by adding *dsr*AB gene sequences from since then published metagenomes, as well as closest BLAST hit to *dsr*B gene sequences detected in Lake Cadagno. The phylogenetic annotation was based on a *dsr*AB gene bootstrap tree that was built by ARB Neighbor-Joining with Jukes-Cantor correction using diverse *dsr*AB reads that covered the entire *dsr*B gene amplicon sequence and were at least 750 bp in length. The shorter amplicon sequences from Lake Cadagno, as well as closest BLAST hits that were <750 bp long, were added using the ARB Parsimony option combined with a newly designed, amplicon-specific *dsr*B filter that removed hypervariable regions.

3. RESULTS

3.1 Sulfur Geochemistry in Lake Cadagno sediments

The complete sedimentary sequence from Lake Cadagno is approximately 950 cm long, covering a period of ~13.5 ky (Berg et al., 2022). Sediments are characterized by relatively fine grained pelagic lacustrine sediments intercalated with frequent coarser-grained flood- and mass movement-derived deposits containing remobilized littoral lake and terrestrial sediment in the upper 790 cm, underlain by light-colored fine-grained deposits of late glacial origin (Fig. 1). The sediment can thus be divided into three distinct lithostratigraphic units representing an early oxic lake (950-790 cm; 13.5 to 12.5 kya), a redox transition interval (790-760 cm; 12.5 to 10.9 kya), and the euxinic period (above 760 cm; 10.9 kya to present). High-resolution mapping of element geochemistry on split core surfaces (Fig. 1) reveals that the accumulation of sulfur is

restricted to sediments deposited after the onset of periodic anoxia (transition interval) to permanently reducing conditions (euxinic interval). Fe and S were normalized against Ti, which represents the lithogenic fraction unaltered by redox processes in the aquatic environment. The correlation between S/Ti and Fe/Ti suggests the presence of authigenic iron sulfide phases. The largest S excursions are located at 300, 560, and 637, which correspond to lacustrine deposits according to the lithological sequence.

Figure 1| Lithological profile determined from a composite core image of the sedimentary sequence retrieved from Lake Cadagno. XRF profiles of S/Ti and Fe/Ti from Berg et al (2022). Changes in lake redox chemistry are denoted by dashed lines.

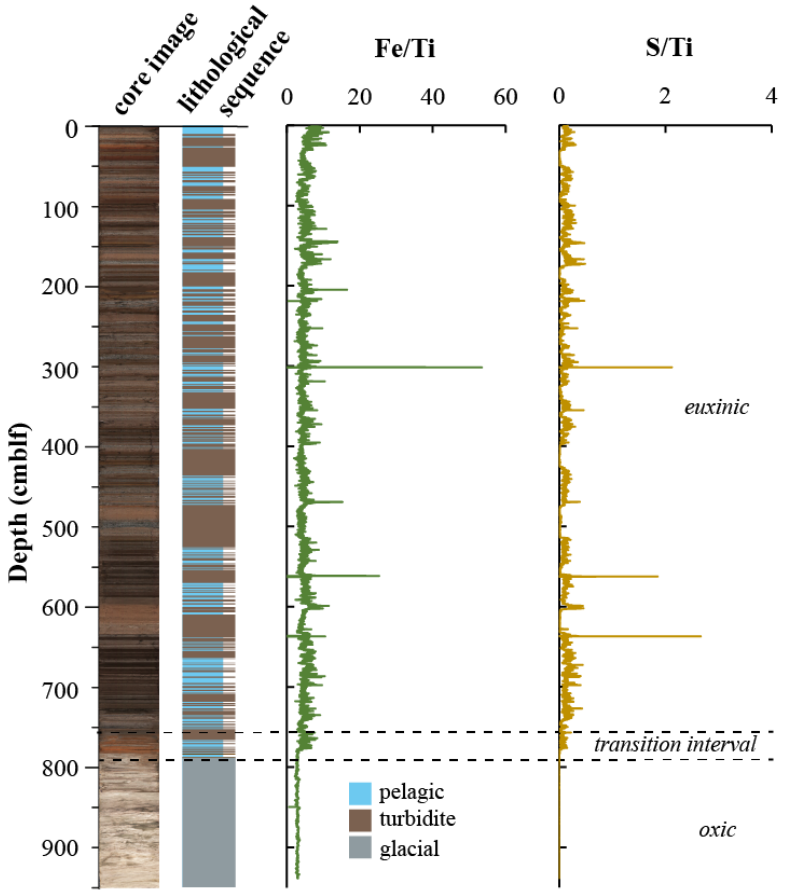

To obtain further insights into sulfur redox cycling in these sediments, major solid sulfur phases were quantified (Fig. 2A). Elemental sulfur (S^0) is the most abundant solid sulfur phase in surface sediments at 300 µmol/g dry sediment. The parallel decrease in S^0 and Fe^{III} (Fig. 2B) with depth indicate increasingly reducing conditions. Both AVS (mostly amorphous FeS and mackinawite) and HAS exhibit a peak at 10 cm depth, which coincides with a peak in dissolved Fe^{2+} and the steepest decrease in sulfate concentrations (Fig. 2C). Below this depth, AVS, HAS, and S^0 decrease in parallel with sulfate at the expense of CRS formation. Most carbon is in organic form in the Lake Cadagno sediments, with measurable contributions (<2 wt%) of total

Figure 2| Geochemistry of (A) major solid-phase sulfur pools along with (B) FeIII and total organic and inorganic carbon and (C) dissolved species involved in sulfur cycling in the surface sediments of Lake Cadagno. (D) Isotope ratios of major sulfur pools with data from 1991 represented as open symbols overlain on profiles from 2019. The shaded region indicates the sulfate depletion zone.

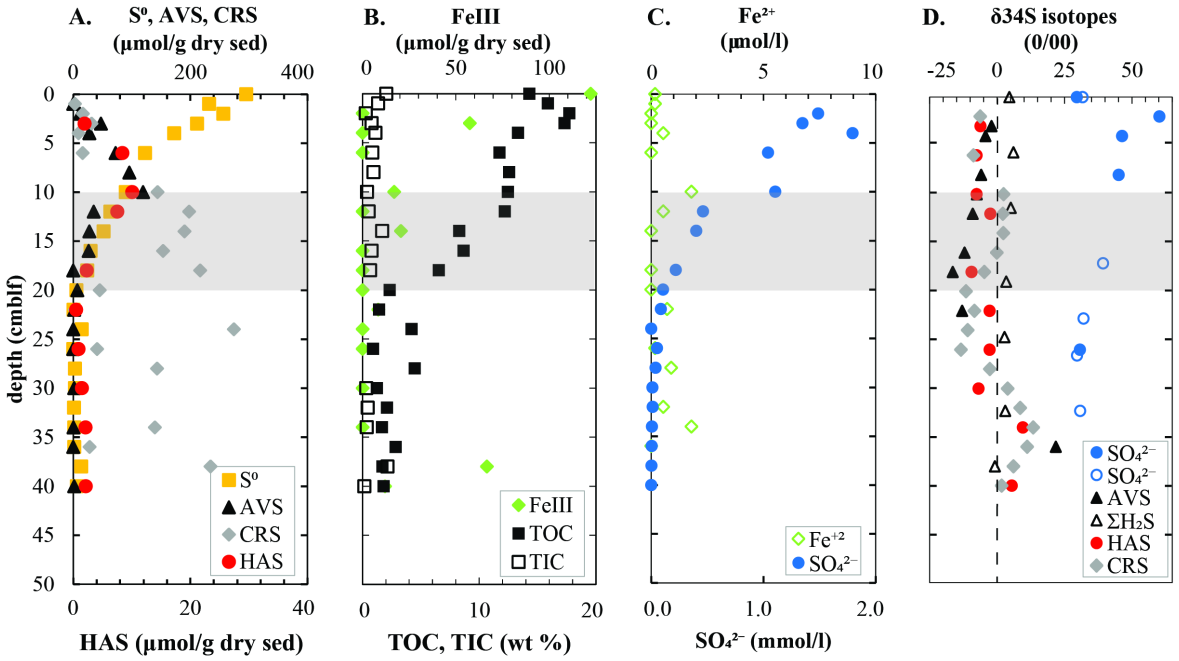

inorganic carbon (TIC) present only in the top few centimeters and again at 14 cm depth (Fig. 2B).

Notably, $\delta^{34}S$ sulfate profiles measured more than 30 years apart coincide surprisingly well (Fig. 2D). Sulfate in the upper sediments is highly enriched in ^{34}S, increasing from +24 ‰ in the bottom waters to +60 ‰ within the upper 2 cm. This zone coincides with strong decreases in TOC and isotopically light ^{13}C-DIC values where high rates of organic matter mineralization have been inferred (Berg et al., 2022; Gajendra et al., 2023). There is a small but consistent offset between $\delta^{34}S$ in reduced sulfur pools of H_2S, AVS, HAS and CRS but no real trends. The widest fluctuations of $\delta^{34}S$ values were measured in the AVS with -16 ‰ at +16 cm and 22‰ at 34 cm depth.

In mid-column sediments between 150 and 760 cm, S^0 and AVS are barely or not detectable whereas HAS concentrations are relatively constant (0.42 - 4.40 µmol/g dry sed) and

CRS levels fluctuate widely (0-270 µmol/g dry sed). The highest concentrations of CRS and HAS are associated with lacustrine deposits (Fig. 3A; see also Supplementary Tables 1&2). In the deep euxinic sediments, exceptionally high CRS contents were detected in a handful of samples that are typically lacustrine deposits and follow broadly the same trend as solid FeIII and dissolved Fe^{2+} concentrations (Fig. 3B,C).

At 760 cm, a second SDZ has been described based on an upwards-diffusing gradient of sulfate thought to originate from a subterranean aquifer (Berg et al., 2022). The change in redox conditions at 775 cm depth is marked by a small peak in AVS (9 µmol/g dry sed) and S^0 (23 µmol/g dry sed). In concurrence with extant oxidizing conditions, late glacial sediments below 790 cm are poor in reduced sulfur and organic matter but contain measurable iron oxides and up to 0.2 mmol/l sulfate in porewaters (Fig. 3B,C). These sulfate concentrations are much

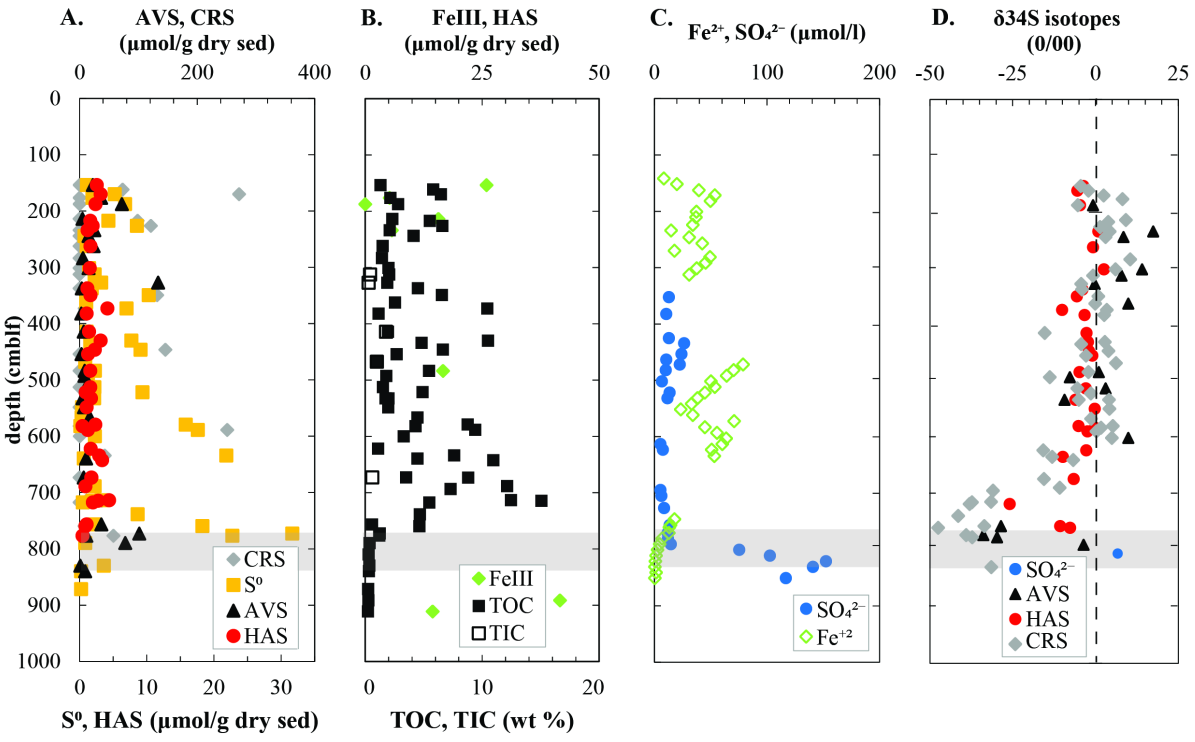

Figure 3| Geochemistry of (A) major solid-phase sulfur pools along with (B) FeIII and total organic and inorganic carbon and (C) dissolved species involved in sulfur cycling in the deep sediments of Lake Cadagno. (D) Isotope ratios of major sulfur pools. Note that sufficient porewater was obtained to measure sulfate isotopes by pooling five deep sediment samples and are thus an average value. The shaded region indicates the sulfate depletion zone.

lower than concentrations of sulfate in lake bottom water (1.8 mmol/l), but in the same general range as a subaquatic spring (0.27 mmol/l) and a surface spring (0.17 mmol/l).

Sufficient sulfate for isotopic analyses could only be obtained by pooling porewater from the entire late glacial sediment sequence (790-910 cm). This averaged sulfate isotopic signature is relatively light (+7‰; Fig. 3D), which is more similar to values measured in subaquatic (+12‰) and surface (+15‰) springs. Isotopic values of reduced sulfur pools fluctuate between positive and negative values with no discernible trend in the mid-column sediment from 150-600 cm depth. In the deep SDZ, δ^{34}S-AVS becomes strongly negative, exhibiting values as low as -34‰ coinciding with lighter porewater sulfate (+6.8‰). CRS is more depleted in ^{34}S than AVS in this zone, with extremely light values of -47.5‰ at 760 cm which is equivalent to a fractionation of 54‰ compared to deep porewater sulfate. δ^{34}S-HAS are consistently less negative than AVS and CRS, varying between 0‰ and -26‰ down to 750 cm depth in respective sediment layers. No significant difference in HAS isotopic composition was found between sediment layer types.

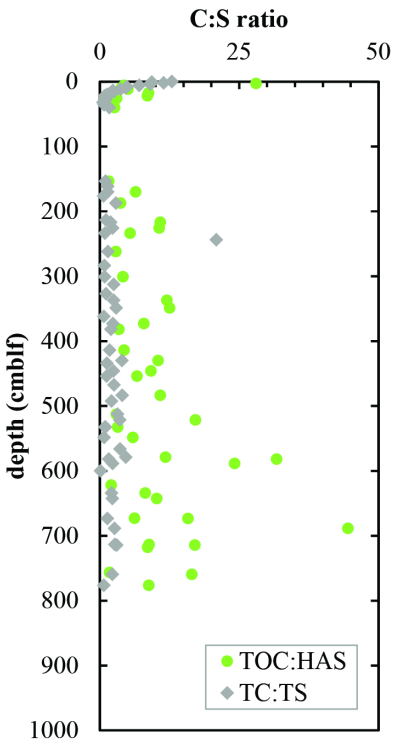

Figure 4| Ratios of total organic carbon:humic acid sulfur (TOC:HAS) and total carbon:total sulfur (TC:TS).

C to S ratios of organic matter are expected to decrease when sulfide reacts with organic matter to form organic S, or when microorganisms preferentially degrade organic carbon and leave behind organic S. TC:TS decreases from 12 at the surface to about 1.3 at 20 cm depth and remains relatively constant throughout the deeper sediments (Fig. 4). Most of this carbon is in organic form, with measurable contributions of total inorganic carbon (TIC) present only in

surface sediment and again at 400 cm depth (<2 wt%; Fig. 2B). The apparent outlier at 243 cm is due to very low sulfur concentrations measured in this sample. A part of the total organic sulfur could be measured as HAS, and the ratios of TOC:HAS exhibit decrease from the surface to 25 cm depth (Fig. 4). Below 150 cm depth, ratios of TOC:HAS fluctuate widely, following the same trend as TOC (r^2= 0.31) with an even stronger correlation (r^2= 0.81) among terrestrial sediments only. In fact there is a significant difference ($p < 0.0001$) in TOC:HAS ratios between sediment layers of lacustrine and terrestrial origin (student's t-test).

3.2 Genetic potential for microbial sulfur cycling

Abundances of sulfur-cycling microorganisms in the Lake Cadagno sediment column were assessed by qPCR of functional genes for sulfate reduction (*dsr*B) and sulfur oxidation (*sox*B) (Fig. 5). Copy numbers of *dsr*B gradually decrease from surface sediments (4.23×10^8 copies/g wet sediment) to the upper SDZ (7.17×10^6 copies/g, 44 cm depth). Throughout the SDZ (35 cm and below), gene copy numbers remain relatively stable between 1.58×10^6 and 2.9×10^7 copies/g wet sediment. Within the lower sulfate-methane depletion zone at around 810 cm depth, *dsr*B copy numbers drop off greatly, to values of 10^1 and 3.10×10^3 and copies/g before increasing again to 2.77×10^4 copies/g in parallel with increasing sulfate concentrations in the underlying oxic, glacial interval (Fig. 5; also see Fig. 2C).

Surprisingly, *sox*B was detectable throughout the entire sediment column. Highest values (up to 6.45×10^3 copies/g sediment) were found in the sulfate-rich surface sediments down to the SDZ. In mid-column sediments, sulfur oxidation gene copies were much lower (1.84×10^0 -1.93×10^2 copies/g) before increasing again in the lower SDZ and reaching a second peak in the glacial sediment layer (6.59×10^3 copies/g). This increase in sulfur oxidation potential matches the oxidizing, and most likely oxic, conditions in this deep glacial sediment layer that are by the presence of Fe-oxides, elemental sulfur, and sulfate (Fig. 3A-C). Sulfur

Figure 5| Depth profiles of *dsr*B and *sox*B gene copy numbers. Copies of both genes were detectable by qPCR in all samples targeted. Shaded gray regions indicate sulfate-methane depletion zones.

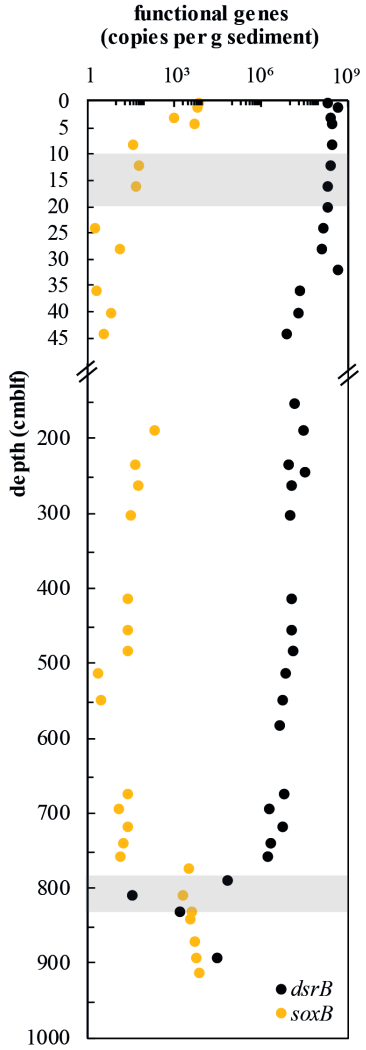

oxidizing bacteria appear to make up a large part of the total microbial population in this layer, with an average ratio of *sox*B to 16S DNA copies/g sediment of 1.17 ± 1.34. At the same time, 16S qPCR data indicate a drop in microbial population size from 10^8 copies/g sediment in the lower SDZ to 10^3 to 10^5 copies/g in the deep glacial layer (Berg et al., 2022).

3.3 Diversity of sulfate-reducing microorganisms

Sequencing of the sulfate reduction gene (*dsr*B) revealed a diverse assembly of potential sulfate reducers in Lake Cadagno sediments (Fig. 6). The majority of sequences could not be classified beyond the supergroup level, indicating that they belong to novel lineages. Overall, the sulfate reducers identified in our gene amplicon libraries were consistent with those identified in 16S rRNA gene libraries, with high relative abundances of Deltaproteobacteria, Nitrospirae, and Chloroflexota (Berg et al., 2022). The community profile shows a clear differentiation between surface sediment and deeper sulfate-depleted layers, and there is a net decrease in taxonomic diversity with depth and sediment age.

Similar to other sulfate-rich sedimentary environments, Lake Cadagno surface sediments harbor highly abundant (>80% relative abundance) Desulfobacterota (formerly Deltaproteobacteria). Most of these belong to uncultured members of the order Desulfobacterales, clade Schlöppnerbrunnen I + II (originally identified in peatland soils), and

other unclassified Deltaproteobacteria. In addition, reads belonging to the genus *Desulfomonile*, of which members are known to also disproportionate sulfur intermediates (Slobodkin and Slobodkina, 2019), are well represented in sediments between 4 cm and 28 cm below the sediment surface (2%-8% of the total community).

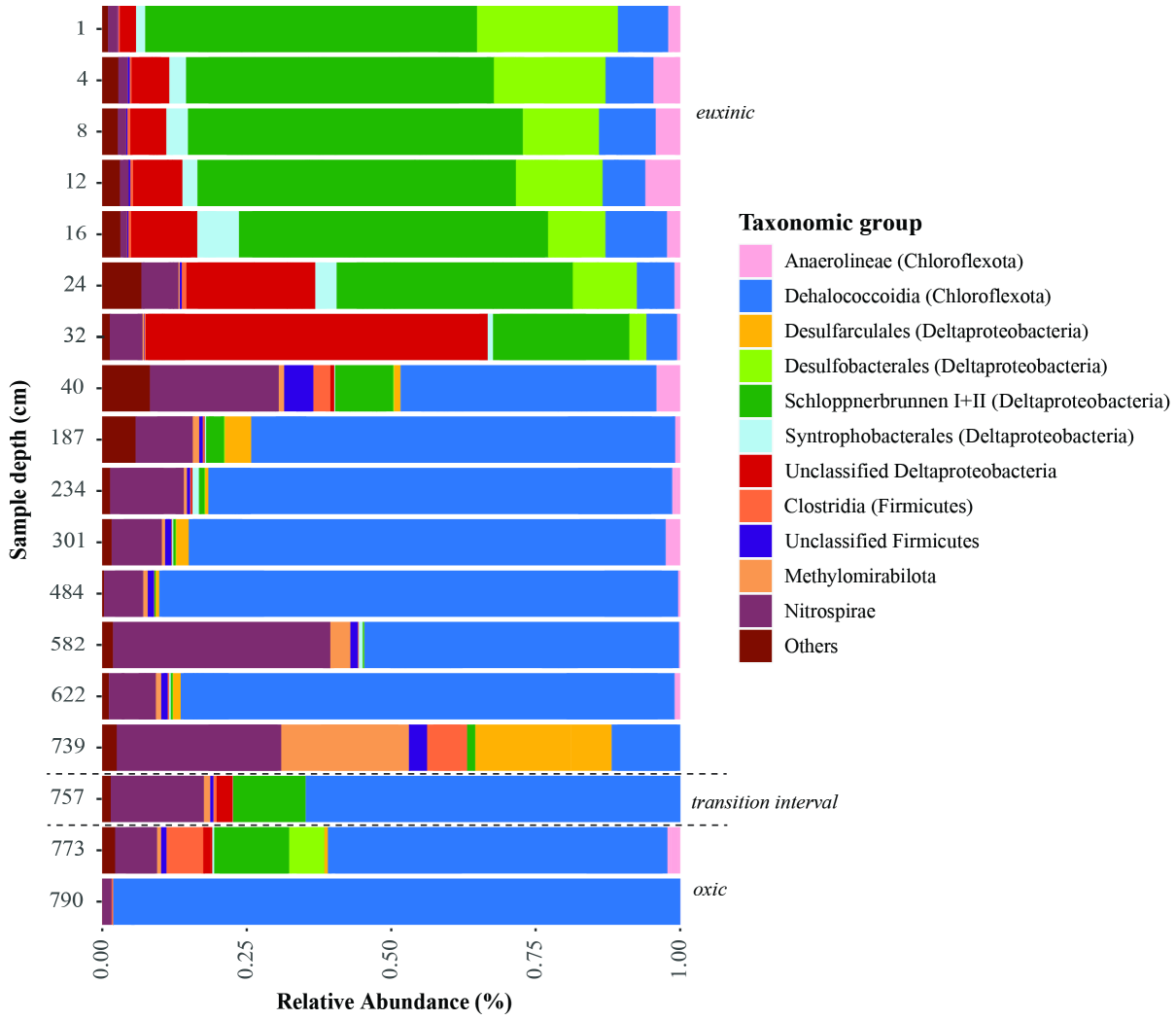

Figure 6| Taxonomic classification of functional genes *dsrB* recovered from the Lake Cadagno sediment depth. Sediment geological transitions are indicated with dashed lines.

Below the SDZ at 40 cm there is a shift in the sulfate-reducing microbial assemblage toward the dominance of uncultivated Chloroflexota. A second compositional shift occurs in deeper layers around the redox transition interval at 739 cm depth. Genes for sulfate reduction in these layers affiliate with Clostridiales, Dehalococcoidia, Methylomirabilales, and the phylum Nitrospirae. Sulfate reducers belonging to Desulfobacterota also reappear close to the

363 redox transition but are distinct from those in surface sediments, affiliating mostly with the
364 species *Desulfoarculus baarsii* (classified within the order Desulfarculales). In the deep glacial
365 sediment (> 790 cm), the diversity of microbial sulfate-reducers is reduced (98% of *dsr*B
366 sequence reads) to Chloroflexota from the classes Anaerolineae and Dehalococcoidia.

367 **4. DISCUSSION**

368 ***4.1 Cycles of sulfate reduction and sulfide oxidation drive isotope fractionation in both***
369 ***surface and deep sediments***

370 The relatively heavy isotopic signature of sulfate in Lake Cadagno bottom waters ($\delta^{34}S$ = +24
371 ‰) compared to the $\delta^{34}S$ of source waters observed in subaquatic +12‰ and surface springs
372 +15‰ indicate active sulfate reduction in the anoxic lower part of the water column. These
373 values are consistent with previously measured values of surface (+12‰) and bottom water
374 (+30‰) sulfate (Canfield et al., 2010). The $\delta^{34}S$ values of sulfate in the Lake Cadagno springs
375 are the same as those of other springs in the Valle Leventina (Steingruber et al., 2020) indicating
376 dissolution of gypsum/dolomite in the marine evaporites from the Middle Triassic ($\delta^{34}S$ circa
377 +15‰) as the main source (Bernasconi et al., 2017).

378 In Lake Cadagno surface sediments (above the first mass movement deposit at 30 cm),
379 the relatively large differences (44 to 66 ‰) in $\delta^{34}S$ between sulfate and CRS are in the same
380 range as those measured in sediment incubations (Canfield et al., 2010). Interestingly, $\delta^{34}S$
381 sulfate profiles measured more than 30 years apart coincide surprisingly well, with sulfate
382 becoming progressively heavier with depth (Fig. 2D) as is typical of closed system sulfate
383 reduction.

384 Microbial sulfur cycling in the sulfate-rich uppermost sediment layer (0-24 cm) appears
385 to be primarily driven by Desulfobacterota. Below this depth, mostly uncultured groups of
386 unclassified Deltaproteobacteria and Dehalococcoida possess an unexplored genetic potential

for sulfate reduction. The high input of labile, microbial organic carbon from the overlying water column supports very high rates of anaerobic organic carbon mineralization within the upper 20 cm (Gajendra et al., 2023). As a result, TOC drops from 15-20 wt. % at the lake floor to values of ≤5 wt. % below 20 cm. Microbial sulfate reduction appears to be primarily linked to the degradation of this organic matter (Berg et al., 2022) though sulfate-driven AOM may additionally occur within the top 2-3 cm (Schubert et al., 2011). Vertical shifts in dominant S-cycling microorganisms from surface sediments (Schloppnerbrunnen I + II, Desulfobacterales (all Desulfobacterota) to Unclassified Desulfobacterota in deeper layers suggest a key influence of sulfate concentrations and organic matter quality on sulfate-reducing microbial community structure. Herein, Desulfobacterales include several known sulfate-reducing and sulfur-disproportionating genera, such as *Desulfobulbus*, *Desulfovibrio*, and *Desulfomonile* (Cypionka et al., 1998; Wasmund et al., 2017; Hashimoto et al., 2022). Similar shifts in dominant sulfate-reducing communities from significant abundances of known groups with cultured representatives in surface layers to dominance of physiologically unclassified taxa in deeper layers have been reported from marine sediments (Jochum et al., 2017). We also detected genes for sulfur oxidation, despite the anoxic nature of these sediments. These genes possibly belong to the facultatively anaerobic bacterial genus *Sulfuricurvum*, which was previously identified in surface sediments (Berg et al., 2022). Sufficient iron oxides (and likely manganese oxides) are also available to drive reoxidation of sulfide to elemental sulfur (Fig. 2A,B).

As sulfate concentrations drop below detection below 30 cm depth, there is a clear shift in dominance from Desulfobacterota to Chloroflexota (Fig. 6). Members of this phylum have so far not been demonstrated to perform dissimilatory sulfur cycling but Chloroflexota *dsrB* sequences have been found in deep sedimentary marine environments (Vuillemin et al., 2020). In the mid-column sediments, *dsr*B gene abundances remain high suggesting that sulfate/sulfur reduction likely continues in sulfate-depleted sediments parallel to fermentation and

412 methanogenic metabolisms. It is possible that sulfate or other oxidized sulfur species, that are
413 regenerated by sulfur oxidation reactions with metal oxides, support these communities of S-
414 cycling microorganisms. Alternatively, the high abundances of Chloroflexota from the class
415 Dehalococcoidia could suggest alternative sulfur-based metabolic activities. Several studies
416 have proposed Chloroflexota to be involved in the metabolism of organic sulfur compounds
417 (Wasmund et al., 2014; Mehrshad et al., 2018), with genomic analyses from deep sea sediments
418 indicating genetic potential for dimethylsulfide, methane sulfonate, and alkane sulfonate
419 metabolisms (Liu et al., 2022). Overall, our findings are consistent with studies of marine
420 sediments demonstrating active sulfate reduction below the zone of sulfate depletion
421 (Holmkvist et al., 2011; Treude et al., 2014; Brunner et al., 2016; Pellerin et al., 2018b) and
422 suggest that deep sulfate reduction also can occur in lake sediments.

423 An oxidizing front and constant groundwater supply of sulfate at the transition between
424 euxinic and deep glacial deposits appears to sustain continuous microbial sulfur cycling at 760-
425 800 cm depth. Pools of reduced sulfur are on average more depleted in $\delta^{34}S$ in the deep glacial
426 sediments than in surface sediments, but the differences between porewater sulfate and HAS
427 ($\varepsilon_{sulfate\text{-}HAS}$ =14-32 ‰), AVS ($\varepsilon_{sulfate\text{-}AVS}$ = 9-45 ‰), and CRS ($\varepsilon_{sulfate\text{-}CRS}$ = 36-53 ‰) in these
428 deep layers are actually smaller. Nonetheless, the values should be taken with caution as only
429 one value of $\delta^{34}S$-sulfate (+7 ‰), representing a pooled average of samples from 790 to 850
430 cm sediment depth, could be measured below 760 cm due to low porewater yields. This
431 relatively light pool of sulfate could represent a mixture of groundwater sulfate (+12 ‰) and
432 sulfate produced through oxidation of sedimentary AVS and CRS by groundwater-derived
433 oxidants. The potential for sulfur oxidation is supported by a strong increase in *sox*B gene
434 copies (Fig. 5), along with the presence of abundant elemental S^0 (Fig. 3A) at the deep redox
435 transition. Light sulfate is likely the main determinant of the highly negative $\delta^{34}S$ values of
436 reduced sulfur.

4.2 Rapid degradation and sulfurization are controlled by organic matter quality

Major changes in solid-phase sulfur pools occur within the upper 20 cm of sediment corresponding to the very high rates of organic matter degradation and microbial sulfate reduction (Berg et al., 2022), These changes include a shift from elemental S and AVS as the dominant S pools at 0-10 cm to CRS (which contains pyrite) as the main S pool between 10-20 cm. This CRS likely derives from chemical reactions of AVS (containing FeS) and elemental sulfur (including polysulfides) (Luther, 1991). Below 20 cm, CRS remains the dominant S pool, and moreover, shows a highly significant ($p < 0.001$) enrichment in lacustrine layers versus mass-movement deposits (student's t-test). The elevated CRS in lacustrine layers confirms the notion that most iron sulfides are of authigenic (rather than terrestrial) origin and result from anaerobic breakdown of lacustrine organic matter driving sulfate reduction.

In addition to CRS formation, we observe the sulfurization of organic matter in these (<100-year-old) surface sediments, as indicated by the strong increase in HAS (up to 10 μmol/g sed) in the top 0-10 cm along with a drop in TOC:HAS ratios (Fig. 4). This observation is consistent with previous studies on Lake Cadagno and other lakes in Switzerland, which reported that most organic matter sulfurization occurs within the initial decades after sediment deposition (Urban et al., 1999; Hebting et al., 2006). Although sulfurized humic acids persist in the older sediment layers, a substantial fraction of the HAS appears to be lost at 10-15 cm depth. The resulting release of sulfide from HAS could explain the more positive δ^{34}S-CRS values despite the concurrent depletion in ^{34}S-sulfate at 10-15 cm sediment depth. This would match previous observations on estuarine sediments, where sulfide released from fulvic acids was shown to contribute to ^{34}S-enriched CRS (Brüchert, 1998).

It is also possible that variations in HAS concentrations are simply due to sediment origin as shown by the strong correlation between TOC:HAS and sediment layer type ($p <$

0.0001). Lacustrine sediment enriched in HAS is interspersed with HAS-poor mass movement deposits containing predominantly terrestrial material beginning at 18-22 cm depth and also forming thicker deposits such as from 31-55 cm depth (Fig. 1). This suggests that fresh lacustrine organic matter from the lake water column is more easily sulfurized than refractory terrestrial organic matter from the lake watershed.

While humic acids comprise only a small part of total organic sulfur in some sediments, they have been shown to be a highly persistent and major component of buried organic carbon (Huc and Durand, 1977). In Lake Cadagno sediments we estimate that an average of 2.6 ± 3.2 % of total organic carbon was extracted as HA and are expected to contain reduced sulfur in the form of organic sulfides or thiols (Ferdelman et al., 1991; Brüchert, 1998; Urban et al., 1999). While sulfurized carotenoids were detected by (Hebting et al., 2006) the chemical composition of most of this sulfurized organic matter remains unclear. It is worth noting that while most lipid-rich algal and microbial material are rapidly degraded in surface sediments, carbohydrates appear to be selectively preserved, thus increasing in contribution to total organic matter in deeper layers (Gajendra et al., 2023). This effective preservation of carbohydrates could be related to macromolecular matrices that are rich in degradation-resistant structural polymers (e.g. hemicelluloses and pectin in microalgal and terrestrial plant biomass; (Gajendra et al., 2023)). In addition, the high chemical reactivity of carbohydrates with hydrogen sulfide could play a role. Past research has shown that carbonyl functional groups are more reactive with inorganic sulfur species than hydroxyl groups, explaining why carbohydrates with a carbonyl group in the C_1 position constitute a major part of sulfurized organic matter in marine sediments (Damsté et al., 1998) and in laboratory experiments (Kok et al., 2000). The same could be the case in deeper sediment layers of Lake Cadagno. Herein sulfurization could even contribute to the effective preservation of carbohydrates in these layers. Alternatively, it is possible that sulfur incorporated into carbohydrates is selectively preserved as organic S

because the surrounding carbohydrate matrices are degradation resistant. Nonetheless, further research is needed to ascertain the extent to which diagenesis has influenced the total organic sulfur pool (e.g., kerogen sulfur and polar bitumen sulfur) and thus carbon preservation over time.

Interestingly, organic sulfur in the deepest part of the Lake Cadagno sediment column (>600 cm sediment depth) is more enriched in $\delta^{34}S$ than co-occurring pyrite. This is consistent with measurements from marine systems (Goldhaber and Kaplan, 1980; Anderson and Pratt, 1995; Brüchert, 1998; Werne et al., 2003; Raven et al., 2016, 2023). Because the fractionation factor of organic matter sulfurization is almost negligible (Amrani and Aizenshtat, 2004), it is likely that differences in the timing of formation explain why the $\delta^{34}S$-HAS in deeper layers is, on average, higher than the $\delta^{34}S$-CRS. HAS may originate in shallow sediment layers, e.g. from ^{34}S-enriched polysulfides produced by partial sulfide oxidation (Putschew et al., 1996; Brüchert, 1998; Werne et al., 2008) and preserve its chemical signature during burial due to high chemical stability. By contrast, groundwater-derived oxidants may cause part of the CRS pool to be re-oxidized and undergo additional fractionation cycles in this deepest sediment layer that directly overlies the aquifer.

CONCLUSION

Here we report the first biogeochemical and isotopic data on sulfur cycling in ancient (up to 13.5 kya) sediments of Lake Cadagno. With its moderate water column sulfate concentrations (2mM), this lake represents an intermediate between typical high-sulfate marine and low-sulfate lake sedimentary environments. In addition to confirming the rapid sulfurization of organic matter, we document two separate zones of reduced sulfur formation within the same sediment column: one close to the surface and a second in deeply buried sediments at the base of the sediment column. This deep sulfate-reduction zone is fed by sulfate-rich, oxidizing

groundwater, which both drives the re-oxidation of sulfides and leaves an isotopic imprint on newly formed reduced sulfur compounds. The deep sulfate reduction zone in Lake Cadagno has parallels to terrestrial aquifers (Porowski et al., 2019), submarine groundwater discharge sites (McAllister et al., 2015) and even deep crustal aquifers (Engelen et al., 2008), within which reworking and overprinting of buried $\delta^{34}S$ by new $\delta^{34}S$ signatures is likely to occur. Deep groundwater-driven sulfur cycling may be more widespread than presently recognized, as submarine groundwater seepage is a common phenomenon and the basaltic ocean crust is the largest aquifer system on Earth.

Deep sulfur cycling in Lake Cadagno appears to be driven by a diverse, and uncultivated biosphere. Most *dsr*B lineages recovered here belong to novel taxa whose role in sulfur and carbon cycling has yet to be revealed. These microorganisms, such as Chloroflexota, are not classical sulfate-reducing bacteria that have been physiologically characterized in the laboratory and much is yet to be understood about their metabolisms. Nonetheless, the recovery of sulfur oxidation genes (*sox*B) from presumably anoxic surface sediments and sulfate reduction genes (*dsr*B) from sulfate-depleted deep sediments opens new questions about deep sources of oxidants which could drive continued sulfur-cycling in such reducing environments.

ACKNOWLEDGEMENTS

We thank the entire 2019 Cadagno sampling crew for assistance in the field, and especially the Alpine Biology Center Foundation (Switzerland) for use of its research facilities. We also acknowledge Iso Christl, Rachele Ossola, and Jorge Spangenberg for their support with chemical analyses. Longhui Deng. was sponsored by the Shanghai Pujiang Program (22PJ1404800). This study was supported by the Swiss National Science Foundation (SNF) grant No. 182096 (M.A.L.).

COMPETING INTERESTS

At least one author is a member of the editorial board of *Biogeosciences*.

DATA AVAILABILITY

*dsr*B gene sequences have been deposited in the NCBI database under Bioproject number PRJNA991470. All other raw data has been deposited in SWISSUbase under study number 20541.

5. AUTHOR CONTRIBUTIONS

JSB performed sediment sampling and chemical analyses, synthesized the data and wrote the manuscript. PCR and LD performed microbial community analyses and interpretations under supervision of CM. SB provided S-isotope data from 1991 and 2019. HV and MM performed sediment sampling and sedimentological characterizations and dating. All co-authors contributed to revision and editing of this manuscript and MAL supervised this project.

REFERENCES

Amrani A. and Aizenshtat Z. (2004) Mechanisms of sulfur introduction chemically controlled: δ34S imprint. *Organic Geochemistry* **35**, 1319–1336.

Anantharaman K., Hausmann B., Jungbluth S. P., Kantor R. S., Lavy A., Warren L. A., Rappé M. S., Pester M., Loy A., Thomas B. C. and Banfield J. F. (2018) Expanded diversity of microbial groups that shape the dissimilatory sulfur cycle. *ISME J* **12**, 1715–1728.

Anderson T. F. and Pratt L. M. (1995) Isotopic Evidence for the Origin of Organic Sulfur and Elemental Sulfur in Marine Sediments. In *Geochemical Transformations of Sedimentary Sulfur* ACS Symposium Series. American Chemical Society. pp. 378–396.

Baloza M., Henkel S., Geibert W., Kasten S. and Holtappels M. (2022) Benthic Carbon Remineralization and Iron Cycling in Relation to Sea Ice Cover Along the Eastern Continental Shelf of the Antarctic Peninsula. *Journal of Geophysical Research: Oceans* **127**, e2021JC018401.

Berg J. S., Lepine M., Laymand E., Han X., Vogel H., Morlock M. A., Gajendra N., Gilli A., Bernasconi S. M., Schubert C. J., Su G. and Lever M. A. (2022) Ancient and Modern Geochemical Signatures in the 13,500-Year Sedimentary Record of Lake Cadagno. *Frontiers in Earth Science* **9**.

Bernasconi S. M., Meier I., Wohlwend S., Brack P., Hochuli P. A., Bläsi H., Wortmann U. G. and Ramseyer K. (2017) An evaporite-based high-resolution sulfur isotope record of Late Permian and Triassic seawater sulfate. *Geochimica et Cosmochimica Acta* **204**, 331–349.

564 Bowles M. W., Mogollón J. M., Kasten S., Zabel M. and Hinrichs K.-U. (2014) Global rates of marine
565 sulfate reduction and implications for sub–sea-floor metabolic activities. *Science* **344**, 889–
566 891.

567 Bradley A. S., Leavitt W. D., Schmidt M., Knoll A. H., Girguis P. R. and Johnston D. T. (2016) Patterns of
568 sulfur isotope fractionation during microbial sulfate reduction. *Geobiology* **14**, 91–101.

569 Brüchert V. (1998) Early diagenesis of sulfur in estuarine sediments: the role of sedimentary humic
570 and fulvic acids. *Geochimica et Cosmochimica Acta* **62**, 1567–1586.

571 Brunner B., Arnold G. L., Røy H., Müller I. A. and Jørgensen B. B. (2016) Off Limits: Sulfate below the
572 Sulfate-Methane Transition. *Front. Earth Sci.* **4**.

573 Brunner B. and Bernasconi S. M. (2005) A revised isotope fractionation model for dissimilatory
574 sulfate reduction in sulfate reducing bacteria. *Geochimica et Cosmochimica Acta* **69**, 4759–
575 4771.

576 Bryant R. N., Houghton J. L., Jones C., Pasquier V., Halevy I. and Fike D. A. (2023) Deconvolving
577 microbial and environmental controls on marine sedimentary pyrite sulfur isotope ratios.
578 *Science* **382**, 912–915.

579 Canfield D. E., Farquhar J. and Zerkle A. L. (2010) High isotope fractionations during sulfate reduction
580 in a low-sulfate euxinic ocean analog. *Geology* **38**, 415–418.

581 Cypionka H., Smock A. M. and Böttcher M. E. (1998) A combined pathway of sulfur compound
582 disproportionation in Desulfovibrio desulfuricans. *FEMS Microbiology Letters* **166**, 181–186.

583 Damsté J. S. and De Leeuw J. W. (1990) Analysis, structure and geochemical significance of
584 organically-bound sulphur in the geosphere: State of the art and future research. *Organic*
585 *Geochemistry* **16**, 1077–1101.

586 Damste J. S., Kok M. D., Koster J. and Schouten S. (1998) Sulfurized carbohydrates: an important
587 sedimentary sink for organic carbon? *Earth and Planetary Science Letters* **164**, 7–13.

588 Damsté J. S., Kok M. D., Köster J. and Schouten S. (1998) Sulfurized carbohydrates: an important
589 sedimentary sink for organic carbon? *Earth and Planetary Science Letters* **164**, 7–13.

590 David M. B. and Mitchell M. J. (1985) Sulfur constituents and cycling in waters, seston, and sediments
591 of an oligotrophic lake. *Limnology and Oceanography* **30**, 1196–1207.

592 Deng L., Meile C., Fiskal A., Bölsterli D., Han X., Gajendra N., Dubois N., Bernasconi S. M. and Lever M.
593 A. (2022) Deposit-feeding worms control subsurface ecosystem functioning in intertidal
594 sediment with strong physical forcing. *PNAS Nexus* **1**, pgac146.

595 Detmers J., Brüchert V., Habicht K. S. and Kuever J. (2001) Diversity of Sulfur Isotope Fractionations
596 by Sulfate-Reducing Prokaryotes. *Appl. Environ. Microbiol.* **67**, 888–894.

597 Engelen B., Ziegelmüller ,Katja, Wolf ,Lars, Köpke ,Beate, Gittel ,Antje, Cypionka ,Heribert, Treude
598 ,Tina, Nakagawa ,Satoshi, Inagaki ,Fumio, Lever ,Mark Alexander and and Steinsbu B. O.
599 (2008) Fluids from the Oceanic Crust Support Microbial Activities within the Deep Biosphere.
600 *Geomicrobiology Journal* **25**, 56–66.

Ferdelman T. G., Church T. M. and Luther G. W. (1991) Sulfur enrichment of humic substances in a Delaware salt marsh sediment core. *Geochimica et Cosmochimica Acta* **55**, 979–988.

Fike D. A., Bradley A. S. and Rose C. V. (2015) Rethinking the Ancient Sulfur Cycle. *Annual Review of Earth and Planetary Sciences* **43**, 593–622.

Fossing H. and Jørgensen B. B. (1989) Measurement of bacterial sulfate reduction in sediments: Evaluation of a single-step chromium reduction method. *Biogeochemistry* **8**, 205–222.

Gajendra N., Berg J. S., Vogel H., Deng L., Wolf S. M., Bernasconi S. M., Dubois N., Schubert C. J. and Lever M. A. (2023) Carbohydrate compositional trends throughout Holocene sediments of an alpine lake (Lake Cadagno). *Front. Earth Sci.* **11**, 1047224.

Goldhaber M. B. and Kaplan I. R. (1975) Controls and consequences of sulfate reduction rates in recent marine sediments. *Soil Science* **119**, 42.

Goldhaber M. B. and Kaplan I. R. (1980) Mechanisms of sulfur incorporation and isotope fractionation during early diagenesis in sediments of the gulf of California. *Marine Chemistry* **9**, 95–143.

Habicht K. S. and Canfield D. E. (1997) Sulfur isotope fractionation during bacterial sulfate reduction in organic-rich sediments. *Geochimica et Cosmochimica Acta* **61**, 5351–5361.

Hansel C. M., Lentini C. J., Tang Y., Johnston D. T., Wankel S. D. and Jardine P. M. (2015) Dominance of sulfur-fueled iron oxide reduction in low-sulfate freshwater sediments. *ISME J* **9**, 2400–2412.

Hartmann M. and Nielsen H. (2012) δ34S values in recent sea sediments and their significance using several sediment profiles from the western Baltic Sea. *Isotopes in Environmental and Health Studies* **48**, 7–32.

Hashimoto Y., Shimamura S., Tame A., Sawayama S., Miyazaki J., Takai K. and Nakagawa S. (2022) Physiological and comparative proteomic characterization of Desulfolithobacter dissulfuricans gen. nov., sp. nov., a novel mesophilic, sulfur-disproportionating chemolithoautotroph from a deep-sea hydrothermal vent. *Front. Microbiol.* **13**.

Hebting Y., Schaeffer P., Behrens A., Adam P., Schmitt G., Schneckenburger P., Bernasconi S. M. and Albrecht P. (2006) Biomarker Evidence for a Major Preservation Pathway of Sedimentary Organic Carbon. *Science* **312**, 1627–1631.

Holmkvist L., Kamyshny A., Vogt C., Vamvakopoulos K., Ferdelman T. G. and Jørgensen B. B. (2011) Sulfate reduction below the sulfate–methane transition in Black Sea sediments. *Deep Sea Research Part I: Oceanographic Research Papers* **58**, 493–504.

Huc A. Y. and Durand B. M. (1977) Occurrence and significance of humic acids in ancient sediments. *Fuel* **56**, 73–80.

Jochum L. M., Chen X., Lever M. A., Loy A., Jørgensen B. B., Schramm A. and Kjeldsen K. U. (2017) Depth Distribution and Assembly of Sulfate-Reducing Microbial Communities in Marine Sediments of Aarhus Bay. *Appl. Environ. Microbiol.* **83**.

Jørgensen B. B. (1982) Mineralization of organic matter in the sea bed—the role of sulphate reduction. *Nature* **296**, 643–645.

639 Jørgensen B. B., Böttcher M. E., Lüschen H., Neretin L. N. and Volkov I. I. (2004) Anaerobic methane
640 oxidation and a deep H2S sink generate isotopically heavy sulfides in Black Sea sediments 1.
641 *Geochimica et Cosmochimica Acta* **68**, 2095–2118.

642 Kallmeyer J., Ferdelman T. G., Weber A., Fossing H. and Jørgensen B. B. (2004) A cold chromium
643 distillation procedure for radiolabeled sulfide applied to sulfate reduction measurements.
644 *Limnology and Oceanography: Methods* **2**, 171–180.

645 Kaplan I. R. and Rittenberg S. C. Y. 1964 (1964) Microbiological Fractionation of Sulphur Isotopes.
646 *Microbiology* **34**, 195–212.

647 Klein M., Friedrich M., Roger A. J., Hugenholtz P., Fishbain S., Abicht H., Blackall L. L., Stahl D. A. and
648 Wagner M. (2001) Multiple Lateral Transfers of Dissimilatory Sulfite Reductase Genes
649 between Major Lineages of Sulfate-Reducing Prokaryotes. *Journal of Bacteriology* **183**, 6028–
650 6035.

651 Kok M. D., Schouten S. and Sinninghe Damsté J. S. (2000) Formation of insoluble, nonhydrolyzable,
652 sulfur-rich macromolecules via incorporation of inorganic sulfur species into algal
653 carbohydrates. *Geochimica et Cosmochimica Acta* **64**, 2689–2699.

654 Lever M. A., Rouxel O., Alt J. C., Shimizu N., Ono S., Coggon R. M., Shanks W. C., Lapham L., Elvert M.,
655 Prieto-Mollar X., Hinrichs K.-U., Inagaki F. and Teske A. (2013) Evidence for Microbial Carbon
656 and Sulfur Cycling in Deeply Buried Ridge Flank Basalt. *Science* **339**, 1305–1308.

657 Lever M. A., Torti A., Eickenbusch P., Michaud A. B., Šantl-Temkiv T. and Jørgensen B. B. (2015) A
658 modular method for the extraction of DNA and RNA, and the separation of DNA pools from
659 diverse environmental sample types. *Front. Microbiol.* **6**.

660 Liu R., Wei X., Song W., Wang L., Cao J., Wu J., Thomas T., Jin T., Wang Z., Wei W., Wei Y., Zhai H., Yao
661 C., Shen Z., Du J. and Fang J. (2022) Novel Chloroflexi genomes from the deepest ocean
662 reveal metabolic strategies for the adaptation to deep-sea habitats. *Microbiome* **10**, 75.

663 Losher A. (1989) The sulfur cycle in freshwater lake sediments and implications for the use of C/S
664 ratios as indicators of past environmental changes. *Doctoral dissertation, ETH Zurich*.

665 Luther G. W. (1991) Pyrite synthesis via polysulfide compounds. *Geochimica et Cosmochimica Acta*
666 **55**, 2839–2849.

667 Maynard J. B. (1980) Sulfur isotopes of iron sulfides in Devonian-Mississippian shales of the
668 Appalachian basin: control by rate of sedimentation. *Am. J. Sci.; (United States)* **280:8**.

669 McAllister S. M., Barnett J. M., Heiss J. W., Findlay A. J., MacDonald D. J., Dow C. L., Luther III G. W.,
670 Michael H. A. and Chan C. S. (2015) Dynamic hydrologic and biogeochemical processes drive
671 microbially enhanced iron and sulfur cycling within the intertidal mixing zone of a beach
672 aquifer. *Limnology and Oceanography* **60**, 329–345.

673 Mehrshad M., Rodriguez-Valera F., Amoozegar M. A., López-García P. and Ghai R. (2018) The
674 enigmatic SAR202 cluster up close: shedding light on a globally distributed dark ocean
675 lineage involved in sulfur cycling. *ISME J* **12**, 655–668.

676 Meyer B., Imhoff J. F. and Kuever J. (2007) Molecular analysis of the distribution and phylogeny of
677 the soxB gene among sulfur-oxidizing bacteria – evolution of the Sox sulfur oxidation enzyme
678 system. *Environmental Microbiology* **9**, 2957–2977.

679 Mitchell M. J., Landers D. H. and Brodowski D. F. (1981) Sulfur constituents of sediments and their
680 relationship to lake acidification. *Water Air Soil Pollut* **16**, 351–359.

681 Müller A. L., Kjeldsen K. U., Rattei T., Pester M. and Loy A. (2015) Phylogenetic and environmental
682 diversity of DsrAB-type dissimilatory (bi)sulfite reductases. *The ISME Journal* **9**, 1152–1165.

683 Nriagu J. O. and Soon Y. K. (1985) Distribution and isotopic composition of sulfur in lake sediments of
684 northern Ontario. *Geochimica et Cosmochimica Acta* **49**, 823–834.

685 Och L. M. and Shields-Zhou G. A. (2012) The Neoproterozoic oxygenation event: Environmental
686 perturbations and biogeochemical cycling. *Earth-Science Reviews* **110**, 26–57.

687 Orr W. L. and Damsté J. S. (1990) Geochemistry of Sulfur in Petroleum Systems. In *Geochemistry of*
688 *Sulfur in Fossil Fuels* ACS Symposium Series. American Chemical Society. pp. 2–29.

689 Pellerin A., Antler G., Røy H., Findlay A., Beulig F., Scholze C., Turchyn A. V. and Jørgensen B. B.
690 (2018a) The sulfur cycle below the sulfate-methane transition of marine sediments.
691 *Geochimica et Cosmochimica Acta* **239**, 74–89.

692 Pellerin A., Antler G., Røy H., Findlay A., Beulig F., Scholze C., Turchyn A. V. and Jørgensen B. B.
693 (2018b) The sulfur cycle below the sulfate-methane transition of marine sediments.
694 *Geochimica et Cosmochimica Acta* **239**, 74–89.

695 Pester M., Knorr K.-H., Friedrich M. W., Wagner M. and Loy A. (2012) Sulfate-reducing
696 microorganisms in wetlands – fameless actors in carbon cycling and climate change. *Front.*
697 *Microbiol.* **3**.

698 Porowski A., Porowska D. and Halas S. (2019) Identification of Sulfate Sources and Biogeochemical
699 Processes in an Aquifer Affected by Peatland: Insights from Monitoring the Isotopic
700 Composition of Groundwater Sulfate in Kampinos National Park, Poland. *Water* **11**, 1388.

701 Putschew A., Scholz-Böttcher B. M. and Rullkötter J. (1996) Early diagenesis of organic matter and
702 related sulphur incorporation in surface sediments of meromictic Lake Cadagno in the Swiss
703 Alps. *Organic Geochemistry* **25**, 379–390.

704 Raven M. R., Crockford P. W., Hodgskiss M. S. W., Lyons T. W., Tino C. J. and Webb S. M. (2023)
705 Organic matter sulfurization and organic carbon burial in the Mesoproterozoic. *Geochimica*
706 *et Cosmochimica Acta* **347**, 102–115.

707 Raven M. R., Sessions A. L., Fischer W. W. and Adkins J. F. (2016) Sedimentary pyrite δ34S differs
708 from porewater sulfide in Santa Barbara Basin: Proposed role of organic sulfur. *Geochimica*
709 *et Cosmochimica Acta* **186**, 120–134.

710 Rudd J. W. M., Kelly C. A. and Furutani A. (1986) The role of sulfate reduction in long term
711 accumulation of organic and inorganic sulfur in lake sediments1. *Limnology and*
712 *Oceanography* **31**, 1281–1291.

713 Rudnicki M. D., Elderfield H. and Spiro B. (2001) Fractionation of sulfur isotopes during bacterial
714 sulfate reduction in deep ocean sediments at elevated temperatures. *Geochimica et*
715 *Cosmochimica Acta* **65**, 777–789.

716 Schubert C. J., Vazquez F., Lösekann-Behrens T., Knittel K., Tonolla M. and Boetius A. (2011) Evidence
717 for anaerobic oxidation of methane in sediments of a freshwater system (Lago di Cadagno).
718 *FEMS Microbiology Ecology* **76**, 26–38.

719 Schwarcz H. P. and Burnie S. W. (1973) Influence of sedimentary environments on sulfur isotope
720 ratios in clastic rocks: a review. *Mineral. Deposita* **8**, 264–277.

721 Sim M. S., Bosak T. and Ono S. (2011) Large Sulfur Isotope Fractionation Does Not Require
722 Disproportionation. *Science* **333**, 74–77.

723 Slobodkin A. I. and Slobodkina G. B. (2019) Diversity of Sulfur-Disproportionating Microorganisms.
724 *Microbiology* **88**, 509–522.

725 Steingruber S. M., Bernasconi S. M. and Valenti G. (2020) Climate Change-Induced Changes in the
726 Chemistry of a High-Altitude Mountain Lake in the Central Alps. *Aquat Geochem*.

727 Stookey L. L. (1970) Ferrozine---a new spectrophotometric reagent for iron. *ACS Publications*.

728 Treude T., Krause S., Maltby J., Dale A. W., Coffin R. and Hamdan L. J. (2014) Sulfate reduction and
729 methane oxidation activity below the sulfate-methane transition zone in Alaskan Beaufort
730 Sea continental margin sediments: Implications for deep sulfur cycling. *Geochimica et*
731 *Cosmochimica Acta* **144**, 217–237.

732 Urban N. R., Ernst K. and Bernasconi S. (1999) Addition of sulfur to organic matter during early
733 diagenesis of lake sediments. *Geochimica et Cosmochimica Acta* **63**, 837–853.

734 Vuillemin A., Kerrigan Z., D'Hondt S. and Orsi W. D. (2020) Exploring the abundance, metabolic
735 potential and gene expression of subseafloor Chloroflexi in million-year-old oxic and anoxic
736 abyssal clay. *FEMS Microbiology Ecology* **96**, fiaa223.

737 Wasmund K., Mußmann M. and Loy A. (2017) The life sulfuric: microbial ecology of sulfur cycling in
738 marine sediments. *Environmental Microbiology Reports* **9**, 323–344.

739 Wasmund K., Schreiber L., Lloyd K. G., Petersen D. G., Schramm A., Stepanauskas R., Jørgensen B. B.
740 and Adrian L. (2014) Genome sequencing of a single cell of the widely distributed marine
741 subsurface Dehalococcoidia, phylum Chloroflexi. *ISME J* **8**, 383–397.

742 Werne J. P., Lyons T. W., Hollander D. J., Formolo M. J. and Sinninghe Damsté J. S. (2003) Reduced
743 sulfur in euxinic sediments of the Cariaco Basin: sulfur isotope constraints on organic sulfur
744 formation. *Chemical Geology* **195**, 159–179.

745 Werne J. P., Lyons T. W., Hollander D. J., Schouten S., Hopmans E. C. and Sinninghe Damsté J. S.
746 (2008) Investigating pathways of diagenetic organic matter sulfurization using compound-
747 specific sulfur isotope analysis. *Geochimica et Cosmochimica Acta* **72**, 3489–3502.

748 Wirth S. B., Gilli A., Niemann H., Dahl T. W., Ravasi D., Sax N., Hamann Y., Peduzzi R., Peduzzi S.,
749 Tonolla M., Lehmann M. F. and Anselmetti F. S. (2013) Combining sedimentological, trace
750 metal (Mn, Mo) and molecular evidence for reconstructing past water-column redox
751 conditions: The example of meromictic Lake Cadagno (Swiss Alps). *Geochimica et*
752 *Cosmochimica Acta* **120**, 220–238.

753 Wortmann U. G., Bernasconi S. M. and Böttcher M. E. (2001) Hypersulfidic deep biosphere indicates
754 extreme sulfur isotope fractionation during single-step microbial sulfate reduction. *Geology*
755 **29**, 647–650.

756